Supporting information

Gas Chromatography–Trapped Ion Mobility Mass Spectrometry: A Highly Specific and Ultra-Sensitive Platform for Quantifying Sub-ppt Levels of Dioxins and PCBs in Food

Hugo B. Muller, Georges Scholl and Gauthier Eppe*

Mass Spectrometry Laboratory, University of Liège, 4000 Liège, Belgium

Corresponding author
***** Email: g.eppe@uliege.be

TABLES

Tables S1: Concentrations (in pg/μL) of the calibration solutions.

PCDDs	Calibration level					
	1	2	3	4	5	6
2,3,7,8-TCDD	0.05	0.1	0.5	1	5	10
1,2,3,7,8-PeCDD	0.05	0.1	0.5	1	5	10
1,2,3,4,7,8-HxCDD	0.1	0.2	1	2	10	20
1,2,3,6,7,8-HxCDD	0.1	0.2	1	2	10	20
1,2,3,7,8,9-HxCDD	0.1	0.2	1	2	10	20
1,2,3,4,6,7,8-HpCDD	0.1	0.2	1	2	10	20
OCDD	0.25	0.5	2.5	5	25	50

PCDFs	Calibration level					
	1	2	3	4	5	6
2,3,7,8-TCDF	0.05	0.1	0.5	1	5	10
1,2,3,7,8-PeCDF	0.05	0.1	0.5	1	5	10
2,3,4,7,8-PeCDF	0.05	0.1	0.5	1	5	10
1,2,3,4,7,8-HxCDF	0.1	0.2	1	2	10	20
1,2,3,6,7,8-HxCDF	0.1	0.2	1	2	10	20
1,2,3,7,8,9-HxCDF	0.1	0.2	1	2	10	20
2,3,4,6,7,8-HxCDF	0.1	0.2	1	2	10	20
1,2,3,4,6,7,8-HpCDF	0.1	0.2	1	2	10	20
1,2,3,4,7,8,9-HpCDF	0.1	0.2	1	2	10	20
OCDF	0.25	0.5	2.5	5	25	50

NO PCBs	Calibration level					
	1	2	3	4	5	6
TCB 77	0.5	1	2	5	10	20
TCB 81	0.5	1	2	5	10	20
PeCB 126	0.5	1	2	5	10	20
HxCB 169	0.5	1	2	5	10	20

MO PCBs	Calibration level							
	1	2	3	4	5	6	7	8
PeCB 105	0.04	0.1	4	10	20	40	80	140
PeCB 114	0.04	0.1	4	10	20	40	80	140
PeCB 118	0.04	0.1	4	10	20	40	80	140
PeCB 123	0.04	0.1	4	10	20	40	80	140
HxCB 156	0.04	0.1	4	10	20	40	80	140
HxCB 157	0.04	0.1	4	10	20	40	80	140
HxCB 167	0.04	0.1	4	10	20	40	80	140
HpCB 189	0.04	0.1	4	10	20	40	80	140

NDL PCBs	Calibration level								
	1	2	3	4	5	6	7	8	9
TriCB 28	0.04	0.1	4	10	20	40	80	140	500
TCB 52	0.04	0.1	4	10	20	40	80	140	500
PeCB 101	0.04	0.1	4	10	20	40	80	140	500
HxCB 138	0.04	0.1	4	10	20	40	80	140	500
HxCB 153	0.04	0.1	4	10	20	40	80	140	500
HpCB 180	0.04	0.1	4	10	20	40	80	140	500

Table S2: Additional GC parameters (TIMS-TOF instrument).

	Fraction	
	1 MO & NDL PCBs	2 PCDD/Fs & NO PCBs
Gas flow	0.8 mL/min	1 mL/min
Temperature program	• 140°C, held 1 min • 220°C @ 15°C/min, held 7.5 min • 250°C @ 8°C/min • 262°C @ 2°C/min • 310°C @ 15°C/min, held 4.2 min ⇒ Total: 30 min	• 80°C, held 3 min • 200°C @ 70°C/min • 250°C @ 2°C/min, held 7 min • 310°C @ 15°C/min, held 4.3 min ⇒ Total: 45 min

Table S3: GC-APCI source parameters.

Transfer line temperature	300°C
Source temperature	300°C
End plate offset	-500 V
Capillary	-4500 V
Corona	+1000 nA
Nebulizer	2.4 Bar
Dry gas	1.5 L/min
Dry temperature	175°C

Table S4: TIMS parameters.

	Fraction	
	1 MO & NDL PCBs	2 PCDD/Fs & NO PCBs
Accumulation time (duty cycle %)	75 ms (30%$_{dc}$)	250 ms (100%$_{dc}$)
Ramp time (spectra rate)	250 ms (3.9 Hz)	
Accumulation range	Same as analysis range	

Analysis range		Variable (SWIM mode cfr. Figure S2) $\Delta 1/K_0 = 0.07$	Variable (SWIM mode cfr. Figure S2) $\Delta 1/K_0 = 0.06$
Tunnel pressure	Entrance(P1)	3.04 mBar	
	Exit (P2)	0.84 mBar	
	ΔP	2.20 mBar	
IM cell temperature		Not available	
RF voltage		250 V_{pp}	
Transfer voltages	D1	-20 V	
	D2	-120 V	
	D3	50 V	
	D4	20 V	
	D5	0 V	
	D6	100 V	

Table S5: Polysiloxane ions used for mass and ion mobility calibration.

Formula	$1/K_0$ [V.s.cm^{-2}]	CCS [Å^2]	m/z
$[C_6H_{19}Si_3O_3]^+$	0.693	147.2	223.0636
$[C_7H_{21}Si_4O_4]^+$	0.772	162.2	281.0511
$[C_9H_{27}Si_5O_5]^+$	0.827	172.1	355.0699
$[C_{11}H_{33}Si_6O_6]^+$	0.916	189.3	429.0887
$[C_{13}H_{39}Si_7O_7]^+$	-	-	503.1075
$[C_{19}H_{43}Si_7O_6]^+$	-	-	563.1439
$[C_{21}H_{49}Si_8O_7]^+$	-	-	637.1627
$[C_{23}H_{55}Si_9O_8]^+$	-	-	711.1815
$[C_{29}H_{59}Si_9O_7]^+$	-	-	771.2179
$[C_{31}H_{65}Si_{10}O_8]^+$	-	-	845.2367
$[C_{33}H_{71}Si_{11}O_9]^+$	-	-	919.2554

Table S6: qTOF parameters. Three sets of parameters were used at different times during the analysis to optimize the transmission of both lower and higher m/z ions (F1 = PCBs fraction; F2 = dioxins fraction).

	Set 1 F1: Start - 14.6 min F2: Start - 17.0 min	Set 2 F1: 14.6 - 26.6 min F2: 17.0 - 40.4 min	Set 3 F1: 26.6 min - End F2: 40.4 min - End

Funnel 2 RF	200 V_{pp}	250 V_{pp}	300 V_{pp}
Multipole RF	200 V_{pp}	250 V_{pp}	300 V_{pp}
Collision RF	800 V_{pp}	1000 V_{pp}	1200 V_{pp}
Quadrupole energy	8 eV	9 eV	10 eV
Collision cell energy	8 eV	9 eV	10 eV
Collision cell in	190 V	190 V	190 V
Transfert time	55 µs	60 µs	70 µs
Prepulse storage	7 µs	9 µs	11 µs

Tables S7: $^{TIMS}CCS_{N2}$ of the PCDDs, PCDFs and PCBs analysed in this study. The CCS values listed are averages from the calibration solutions 2 to 5.

PCDDs	Average CCS [Å^2] (n=4)	RSD(%)
2,3,7,8-TCDD	159.3	0.04
1,2,3,7,8-PeCDD	165.0	0.04
1,2,3,4,7,8-HxCDD	170.6	0.03
1,2,3,6,7,8-HxCDD	170.6	0.03
1,2,3,7,8,9-HxCDD	168.8	0.03
1,2,3,4,6,7,8-HpCDD	174.4	0.03
OCDD	178.4	0.03

PCDFs	Average CCS [Å^2] (n=4)	RSD(%)
2,3,7,8-TCDF	155.0	0.05
1,2,3,7,8-PeCDF	159.6	0.04
2,3,4,7,8-PeCDF	160.9	0.04
1,2,3,4,7,8-HxCDF	165.1	0.03
1,2,3,6,7,8-HxCDF	165.1	0.00
2,3,4,6,7,8-HxCDF	166.5	0.03
1,2,3,7,8,9-HxCDF	163.2	0.04
1,2,3,4,6,7,8-HpCDF	170.7	0.03
1,2,3,4,7,8,9-HpCDF	168.7	0.03
OCDF	174.3	0.03

NO PCBs	Average CCS [Å^2] (n=4)	RSD(%)
TCB 81	155.7	0.03
TCB 77	156.3	0.03
PeCB 126	162.8	0.00
HxCB 169	169.4	0.03

MO PCBs	Average CCS [Å^2] (n=4)	RSD(%)
PeCB 123	161.3	0.03

PeCB 118	161.9	0.00
PeCB 114	159.9	0.00
PeCB 105	160.4	0.04
HxCB 167	168.2	0.00
HxCB 156	167.0	0.05
HxCB 157	166.7	0.03
HpCB 189	173.2	0.03

NDL PCBs	Average CCS [Å^2] (n=4)	RSD(%)
TriCB 28	148.0	0.06
TCB 52	155.6	0.03
PeCB 101	161.3	0.03
HxCB 153	167.4	0.03
HxCB 138	166.2	0.00
HpCB 180	172.4	0.00

Table S8 – Comparison of calculated mLOQ values using the two approaches: blank-level contamination and instrument LOQ.

Analyte	mLOQ (pg/g) 2g of sample		mLOQ (pg/g) 4g of sample	
	iLOQ	Blank level	iLOQ	Blank level
TCB 81	0.5	2.7	0.25	1.35
TCB 77	0.5	13.1	0.25	6.5
PeCB 126	0.5	0.4	0.25	0.2
PeCB 123	4	5.7	2	2.85
PeCB 118	4	144	2	72
PeCB 114	4	4.8	2	2.4
PeCB 105	4	53.5	2	26.75
HxCB 167	4	1.8	2	0.9
HxCB 156	4	4.0	2	2.0
HxCB 157	4	2.0	2	1.0
HpCB 189	4	0.7	2	0.35
TriCB 28	4	1299	2	649.5
TCB 52	4	2379	2	1189.5
PeCB 101	4	636	2	318
HxCB 153	4	121	2	60.5
HxCB 138	4	68	2	34
HpCB 180	4	15	2	7.5

Table S9: Mean RSD_R and bias measured for the dioxins and PCBs in the different matrices with the two instrumentations.

		Mean RSD_R (% RSD_R <15%) [20% for NDL PCBs]		Mean absolute bias (% |bias| ≤ 20%) [30% for NDL PCBs]	
		TIMS TOF	Sector	TIMS TOF	Sector
PCDD/Fs + NO PCBs	Fish oil	7.0% (100%)	7.3% (100%)	10.5% (88%)	7.9% (100%)
	Palm oil	8.8% (100%)	7.6% (100%)	14.3% (77%)	9.3% (99%)
	Milk fat	10.4% (90%)	3.7% (100%)	13.8% (77%)	5.7% (100%)
	Total	**8.9% (96%)**	**6.1% (100%)**	**13.1% (80%)**	**7.3% (99%)**
MO PCBs	Fish oil	3.9% (88%)	6.3% (100%)	7.8% (98%)	7.2% (100%)
	Palm oil	6.6% (100%)	6.3% (100%)	12.1% (71%)	9.4% (97%)
	Milk fat	3.9% (100%)	3.7% (100%)	7.7% (87%)	5.6% (90%)
	Total	**4.8% (96%)**	**5.4% (100%)**	**8.9% (87%)**	**7.1% (95%)**
NDL PCBs	Fish oil	3.2% (100%)	9.4% (100%)	7.4% (100%)	9.0% (100%)
	Palm oil	4.3% (100%)	7.5% (100%)	7.5% (92%)	13.6% (79%)
	Milk fat	7.5% (100%)	7.5% (100%)	13.0% (89%)	9.4% (100%)
	Total	**5.0% (100%)**	**8.1% (100%)**	**9.8% (93%)**	**10.3% (95%)**

Tables S10: Total WHO_{2005} TEQ concentrations of dioxins (PCDDs + PCDFs) and dioxin like PCBs (NO + MO PCBs) and summed concentrations of NDL PCBs measured by GC-EI-sector and GC-APCI-TIMS-TOF in the different matrices. RSD_R and relative bias values that comply with the criteria from the European Regulation 2017/644 are highlighted in green.

Fish oil	Certified TEQ concentration PT [pg WHO_{2022} TEQ/g_{fat}]	Mean concentration [pg WHO_{2022} TEQ/g_{fat}] (Relative bias %)		RSD_R (%)		Compliance regarding maximum level (EU 2023/915)		
		TIMS	Sector	TIMS	Sector	PT	TIMS	Sector
∑ PCDD/Fs	1.62	1.48 (-8.7)	1.54 (-4.8)	5.0	5.5	Compliant	Compliant	Compliant
∑ DL PCBs	8.57	7.37 (-13.9)	8.49 (-0.39)	1.3	6.4			
∑ PCDD/Fs + DL PCBs	10.19	8.85 (-13.1)	10.03 (-1.5)	0.2	5.9	Non compliant	Non compliant	Non compliant
	Certified concentration PT [ng /g_{fat}]	Mean concentration [ng /g_{fat}] (Relative bias %)		RSD_R (%)				

		TIMS	Sector	TIMS	Sector			
∑ NDL PCBs	100.98	93.79 (-7.1)	100.43 (-0.5)	3.2	9.9	Compliant	Compliant	Compliant

Palm oil	Certified TEQ concentration PT [pg WHO_{2022} TEQ/g_{fat}]	Mean concentration [pg WHO_{2022} TEQ/g_{fat}] (Relative bias %)		RSD_R (%)		Compliance regarding maximum level (EU 2023/915)		
		TIMS	Sector	TIMS	Sector	PT	TIMS	Sector
∑ PCDD/Fs	0.77	0.86 (+11.4)	0.74 (-4.7)	5.8	3.2	Compliant	Compliant	Compliant
∑ DL PCBs	0.36	0.38 (+6.2)	0.39 (+8.6)	2.2	6.4			
∑ PCDD/Fs + DL PCBs	1.13	1.24 (+9.8)	1.13 (-0.5)	5.1	2.4	Compliant	Compliant	Compliant
	Certified concentration PT [ng $/g_{fat}$]	Mean concentration [ng $/g_{fat}$] (Relative bias %)		RSD_R (%)				
		TIMS	Sector	TIMS	Sector			
∑ NDL PCBs	2.53	2.63 (+3.7)	2.86 (+12.9)	3.2	4.5	Compliant	Compliant	Compliant

Milk fat	Certified TEQ concentration PT [pg WHO_{2022} TEQ/g_{fat}]	Mean concentration [pg WHO_{2022} TEQ/g_{fat}] (Relative bias %)		RSD_R (%)		Compliance regarding maximum level (EU 2023/915)		
		TIMS	Sector	TIMS	Sector	PT	TIMS	Sector
∑ PCDD/Fs	2.83	2.68 (-5.2)	2.73 (-3.5)	3.8	1.3	Non compliant	Non compliant	Non compliant
∑ DL PCBs	2.27	2.10 (-7.1)	2.29 (+1.3)	3.7	3.6			
∑ PCDD/Fs + DL PCBs	5.10	4.79 (-6.1)	5.03 (-1.4)	2.7	1.9	Non compliant	Compliant	Non compliant
	Certified concentration PT [ng $/g_{fat}$]	Mean concentration [ng $/g_{fat}$] (Relative bias %)		RSD_R (%)				
		TIMS	Sector	TIMS	Sector			
∑ NDL PCBs	56.88	50.13 (-11.9)	55.11 (-3.1)	6.1	9.5	Non compliant	Compliant	Non compliant

FIGURES

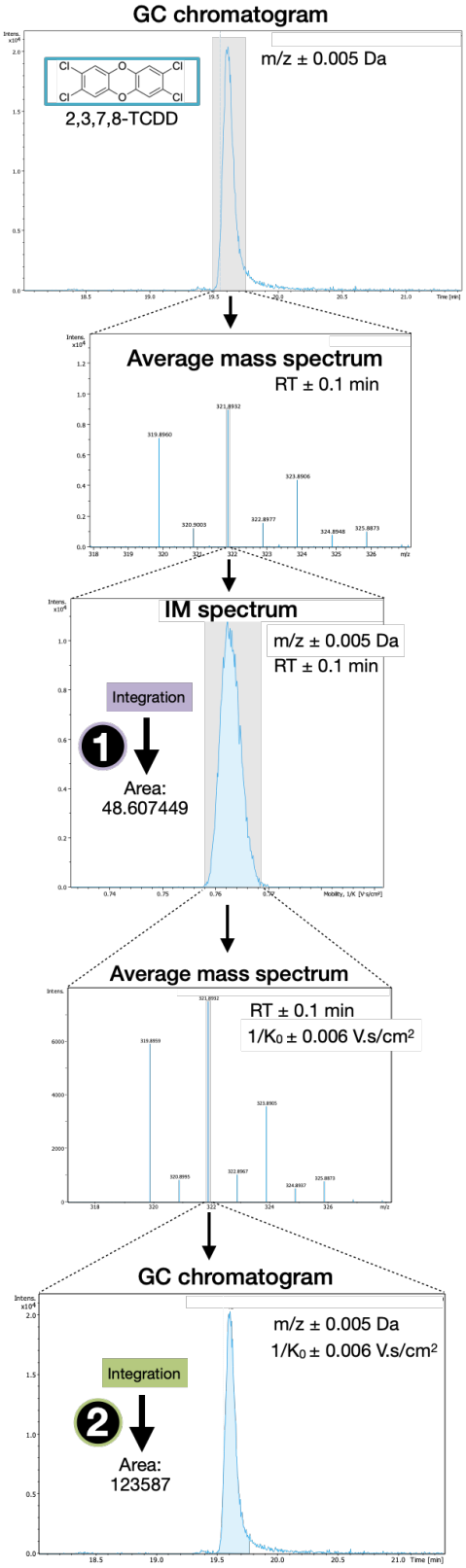

Figure S1: Illustration of the two signal integration procedures that were tested in this study. First, an average mass spectrum was generated over the elution time of the analyte of interest. Then, the ion mobility spectrum of the most intense isotopologue of the isotopic pattern was generated and integrated and the resulting area was used in the quantification process (procedure #1). For the second procedure, an average mass spectrum was generated over the elution time and the ion mobility range of the analyte of interest. A mobility filtered exctracted ion chromatogram was then generated based on this mass spectra. The resulting chromatographic peak was integrated and used in the quantification process (procedure #2).

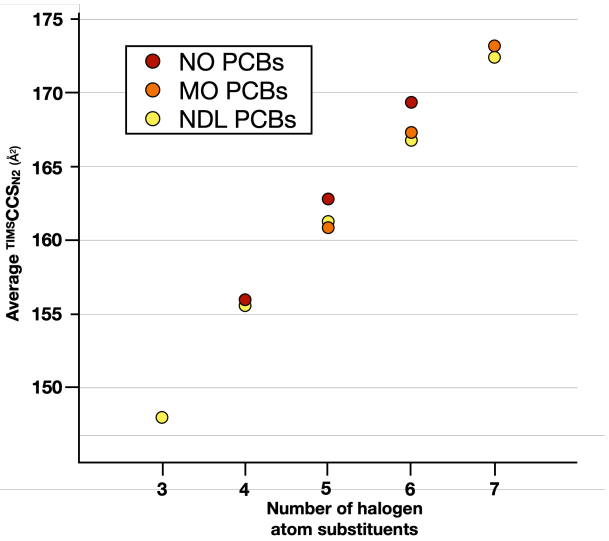

Figure S2: Average CCS of NO, MO and NDL PCBs per halogenation degree.

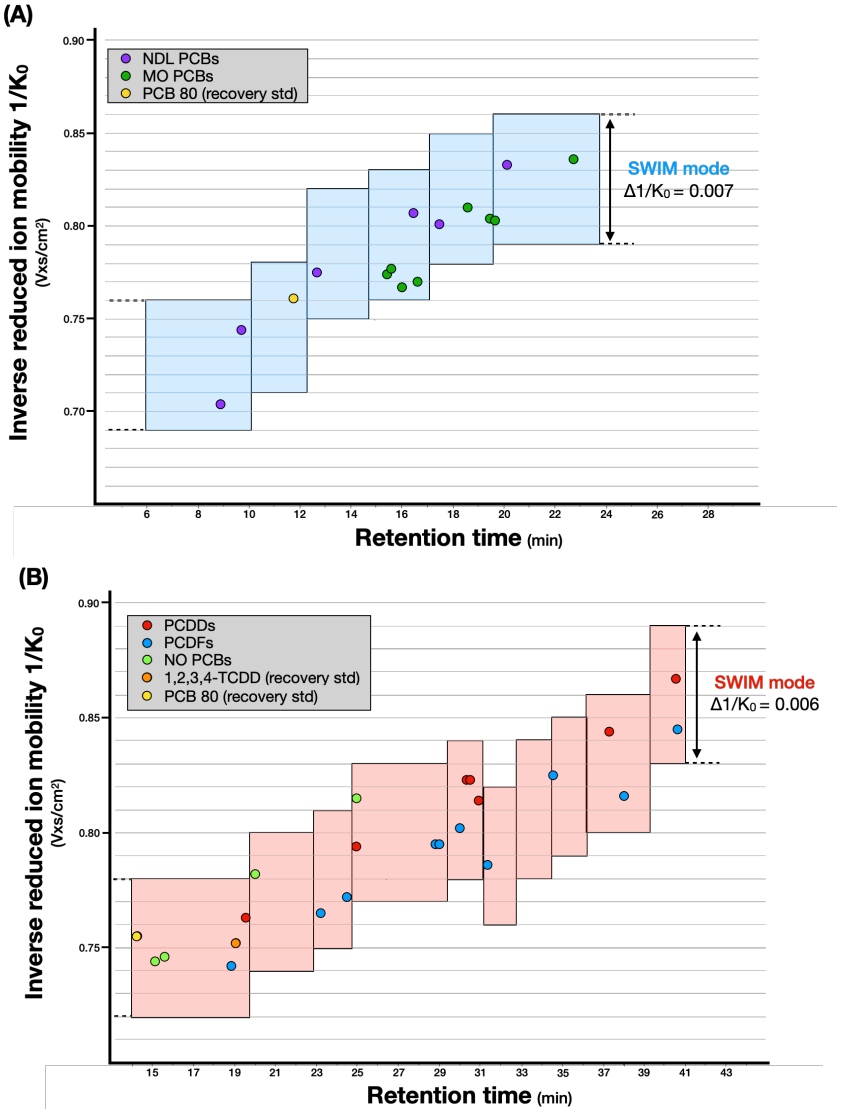

Figure S3: SWIM method applied to (A) the PCBs fraction and (B) the dioxins fraction. The ion mobility range of analysis (represented by the rectangles) is changed during the course of the chromatographic separation to adapt to the CCS of the analytes (represented by the coloured dots) that elute during a given retention time window. This avoids the use of a wider (and therefore less resolvable) ion mobility range that would have been necessary if that range had been constant over time (in order to include all the analytes).

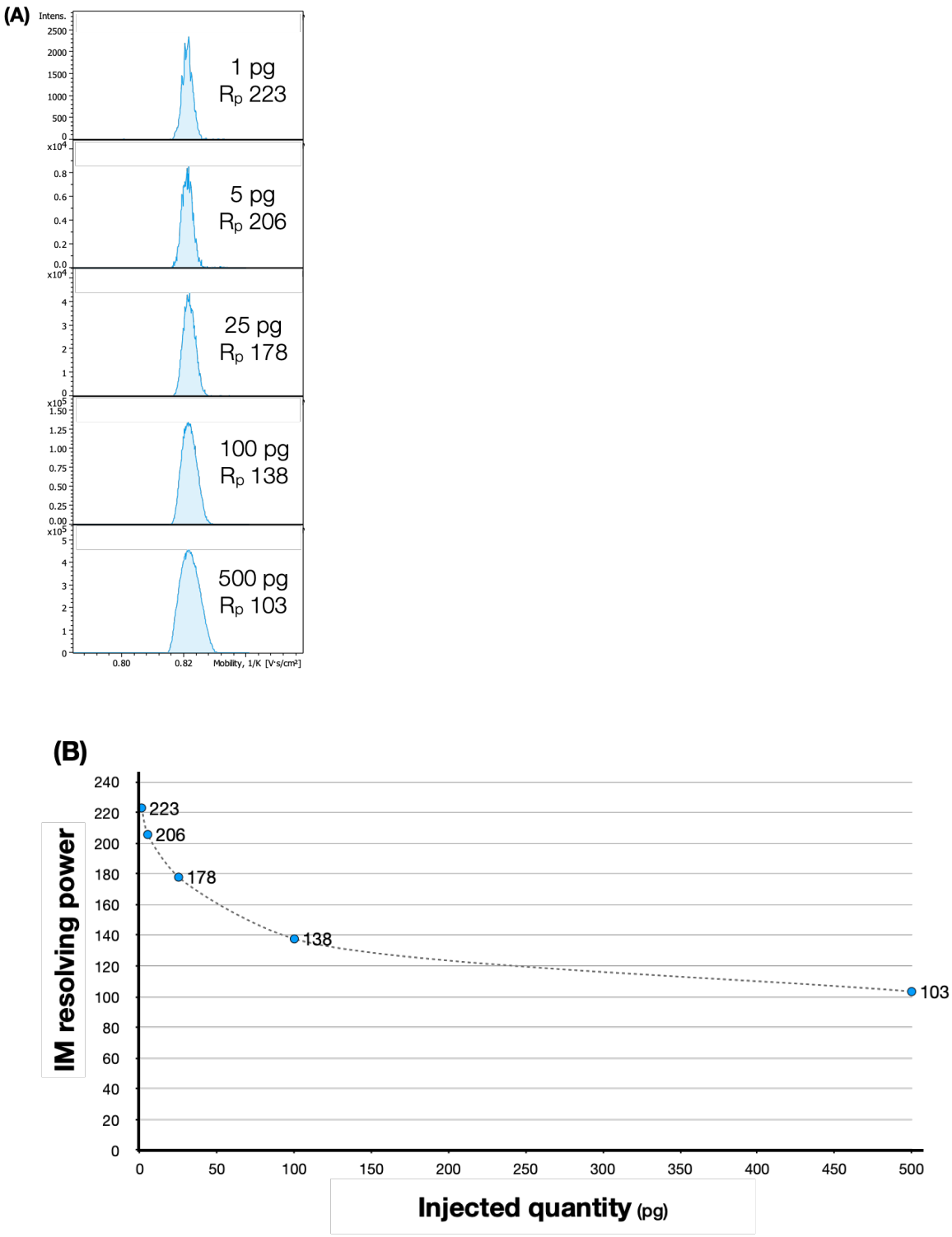

Figure S4: (A) Ion mobility spectra of a tetrabromo diphenylether standard (TBDE 49) analysed in increasing amounts using the PCBs fraction parameters (see Table S4). (B) Plot of resolving power versus injected quantity of TBDE 49 standard demonstrating a significant trend of decreasing resolving power with increasing injected quantity.

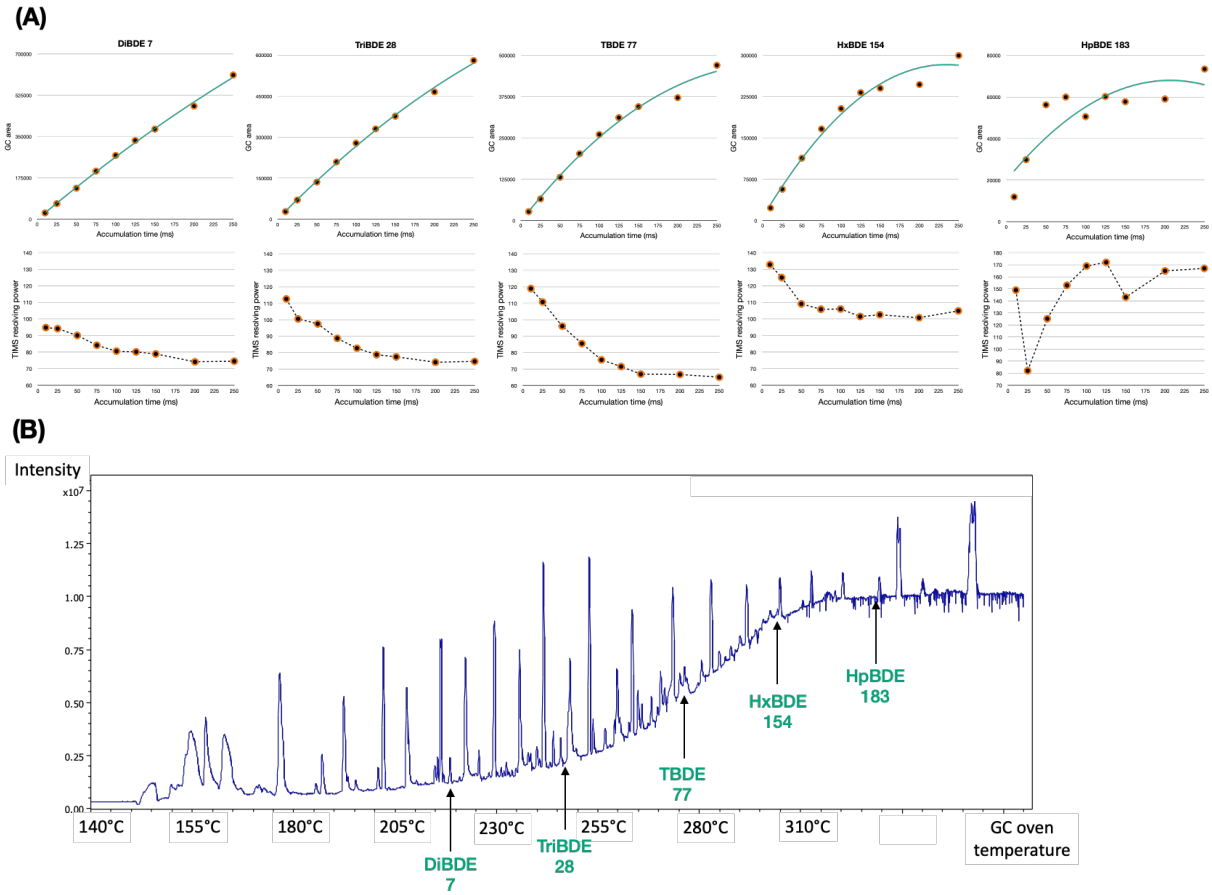

Figure S5: (A) Signal intensity (upper plots) and TIMS resolving power (lower plots) versus accumulation time for five different PBDE standards in positive mode. (B) Total signal intensity (TIC) versus GC oven temperature. The elution temperature of the five PBDE standards is indicated by the corresponding arrows. The series of intense peaks throughout the chromatogram corresponds to artefacts peaks that originate from impurities within the GC system (injector, caps, septa etc.).

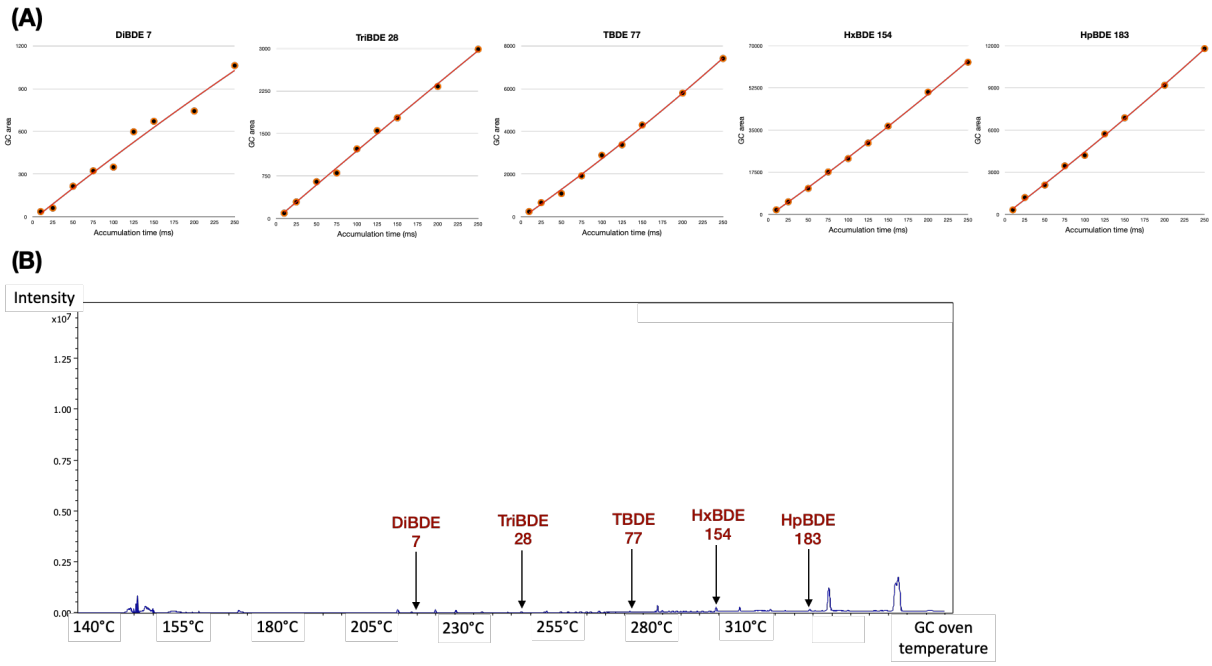

Figure S6: (A) Signal intensity versus accumulation time for the same five PBDE standards in negative mode. (B) Total signal intensity (TIC) versus GC oven temperature. The elution temperature of the PBDE standards is indicated by the corresponding arrows.

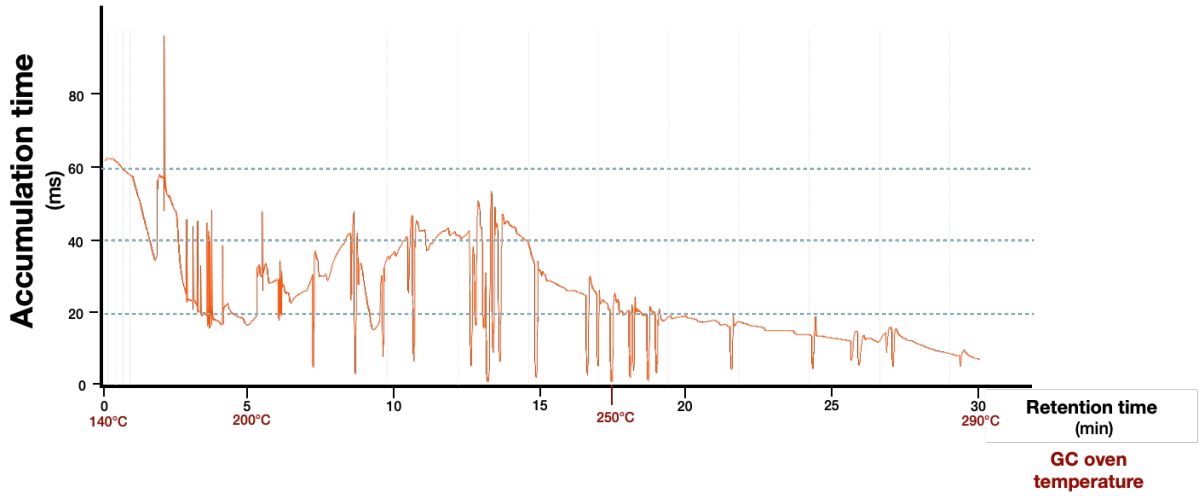

Figure S7: Accumulation time versus retention time and GC oven temperature in ICC mode (7.5 MiO). A slightly modified version of the GC temperature program of the PCBs fraction was used (see Table S2). As can be seen in this figure, the accumulation time already drops to ~60 ms at the start of the GC separation (T=140°C). Between 200 and 250°C, the accumulation time varies between 20 and 50 ms. Above 250°C, it drops below 20 ms and reaches ~10 ms at the end of the separation.

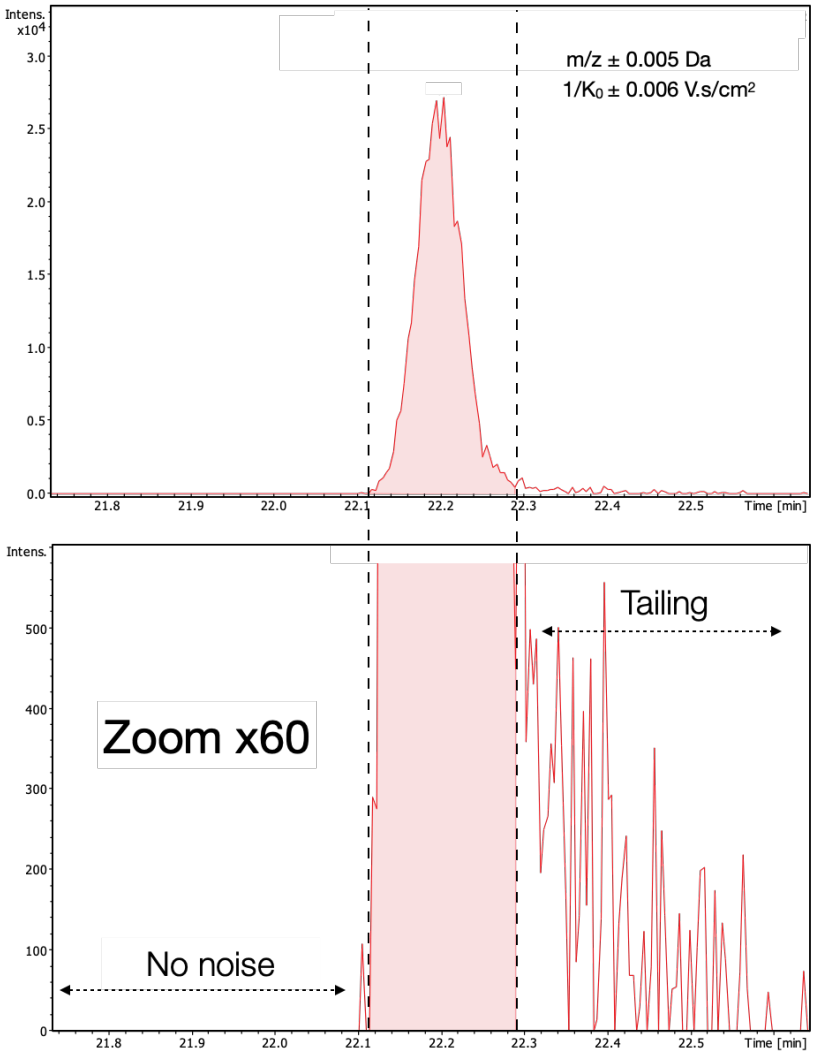

Figure S8: IM-filtered chromatogram of HpCB 189 (4 pg injected) with (lower spectrum) and without (upper spectrum) zoom.

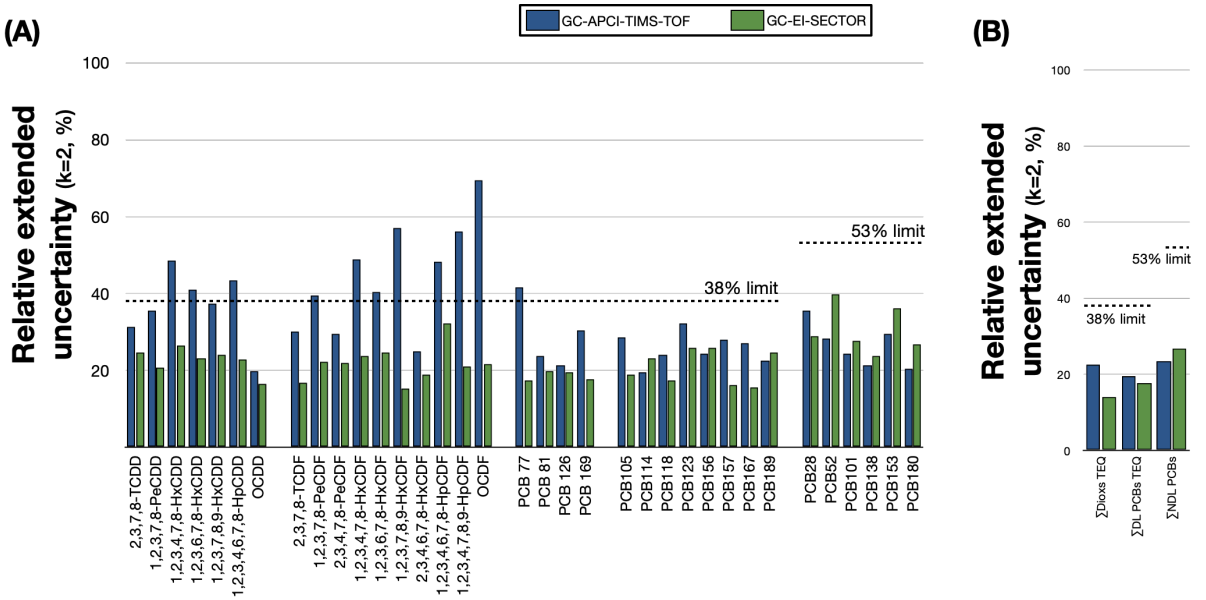

Figure S9: Expanded uncertainty U calculated for the different dioxins and PCBs congeners (A) and the sum TEQ concentrations (B) with the TIMS (blue) and sector (green) methods.

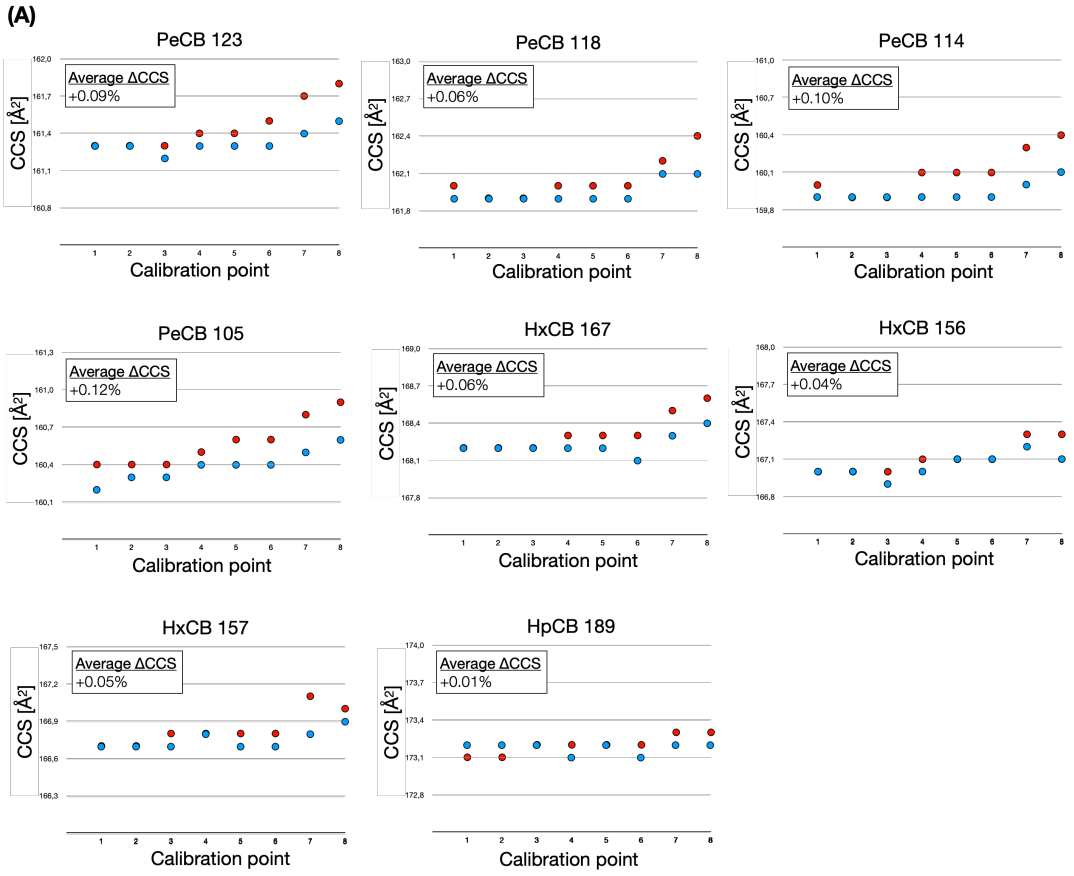

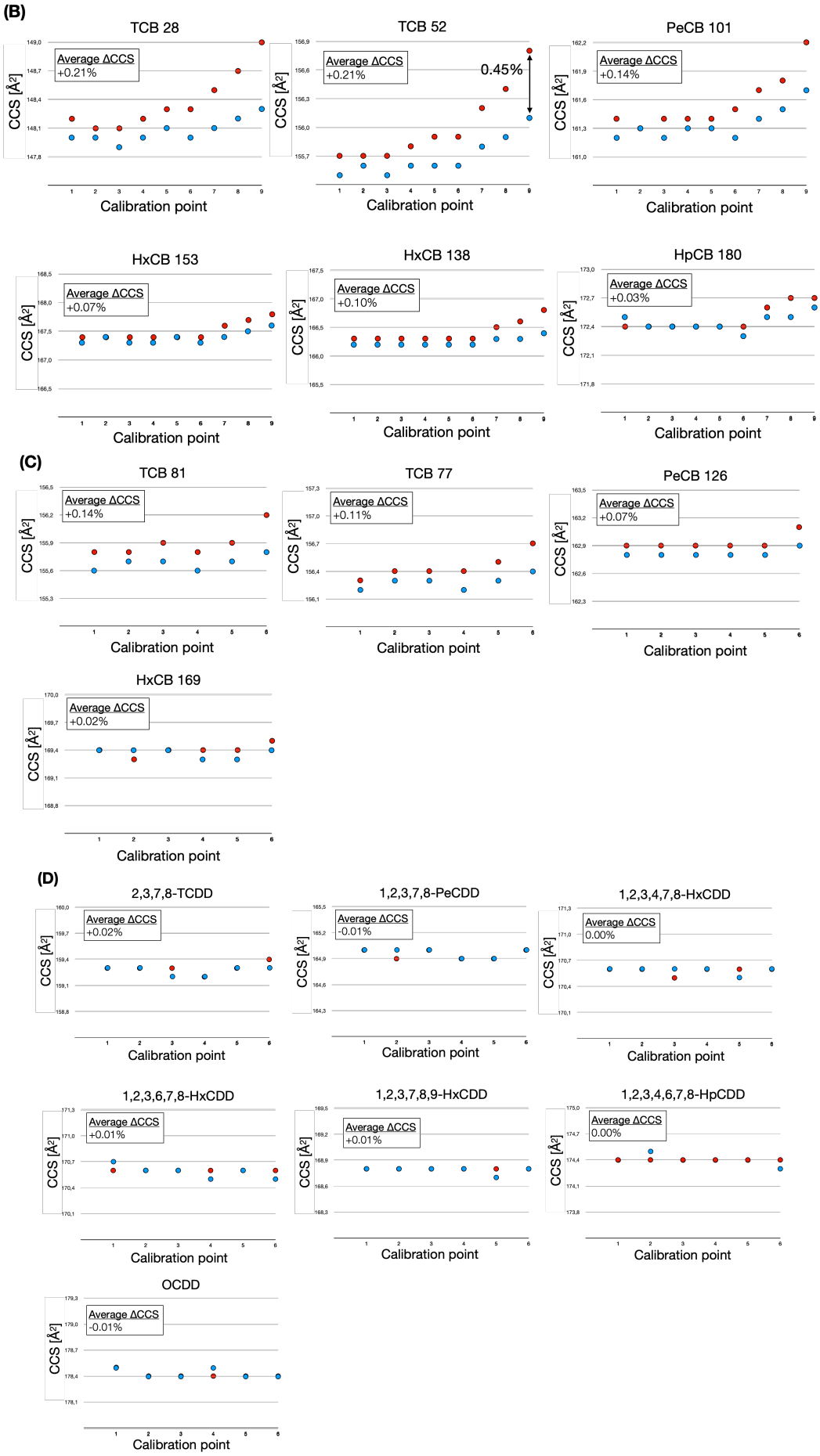
(B)
TCB 28
Average ΔCCS
+0.21%
TCB 52
Average ΔCCS
+0.21%
0.45%
PeCB 101
Average ΔCCS
+0.14%
HxCB 153
Average ΔCCS
+0.07%
HxCB 138
Average ΔCCS
+0.10%
HpCB 180
Average ΔCCS
+0.03%
(C)
TCB 81
Average ΔCCS
+0.14%
TCB 77
Average ΔCCS
+0.11%
PeCB 126
Average ΔCCS
+0.07%
HxCB 169
Average ΔCCS
+0.02%
(D)
2,3,7,8-TCDD
Average ΔCCS
+0.02%
1,2,3,7,8-PeCDD
Average ΔCCS
-0.01%
1,2,3,4,7,8-HxCDD
Average ΔCCS
0.00%
1,2,3,6,7,8-HxCDD
Average ΔCCS
+0.01%
1,2,3,7,8,9-HxCDD
Average ΔCCS
+0.01%
1,2,3,4,6,7,8-HpCDD
Average ΔCCS
0.00%
OCDD
Average ΔCCS
-0.01%
CCS [Å²]
Calibration point

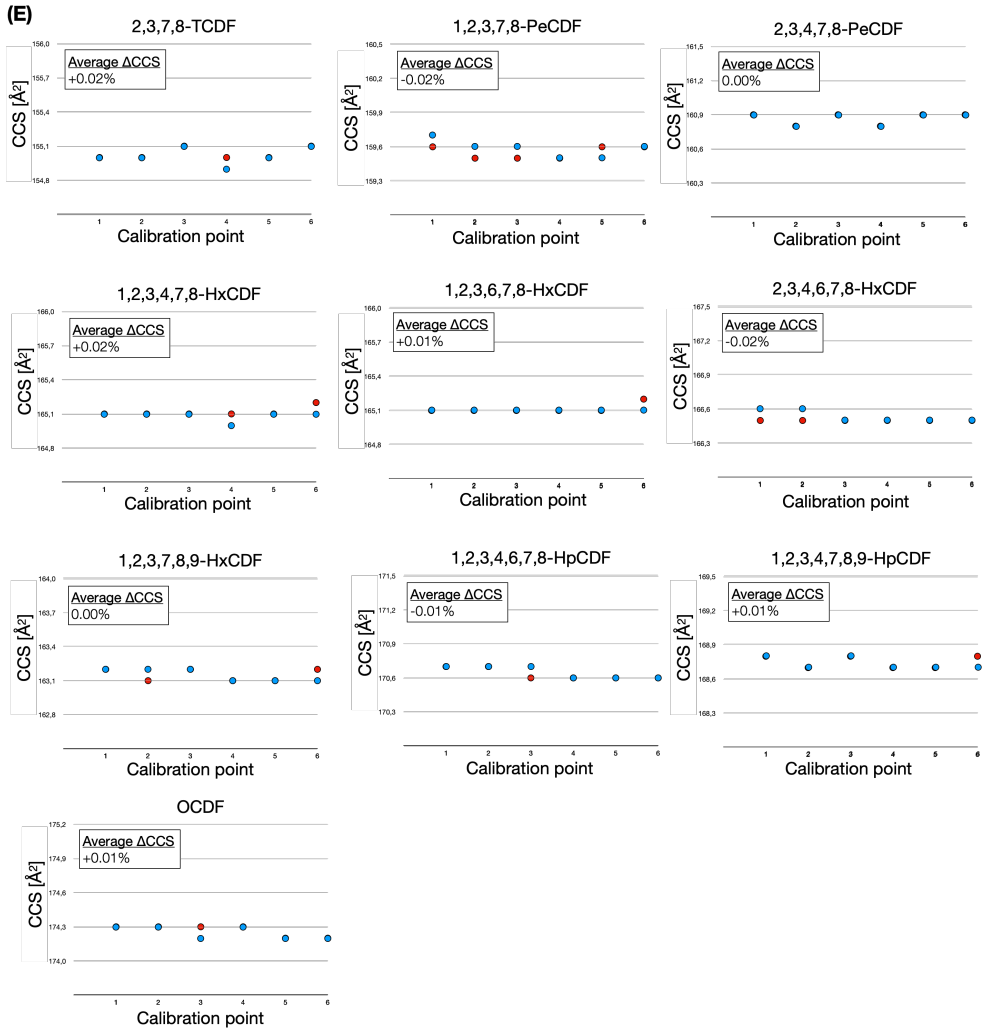

Figure S10: Experimentally measured CCS of both native (blue dots) and ^{13}C isotopically labelled standards (red dots) at the different calibration levels for: (A) MO PCBs; (B) NDL PCBs; (C) NO PCBs; (D) PCDDs and (E) PCDFs. The ΔCCS corresponds to the difference between the CCS value of the ^{13}C and the native standards, expressed as a percentage relative to the CCS of the native standard. The ΔCCS were calculated at each concentration levels and averaged to yield the average ΔCCS value displayed for each analyte in the graphs.

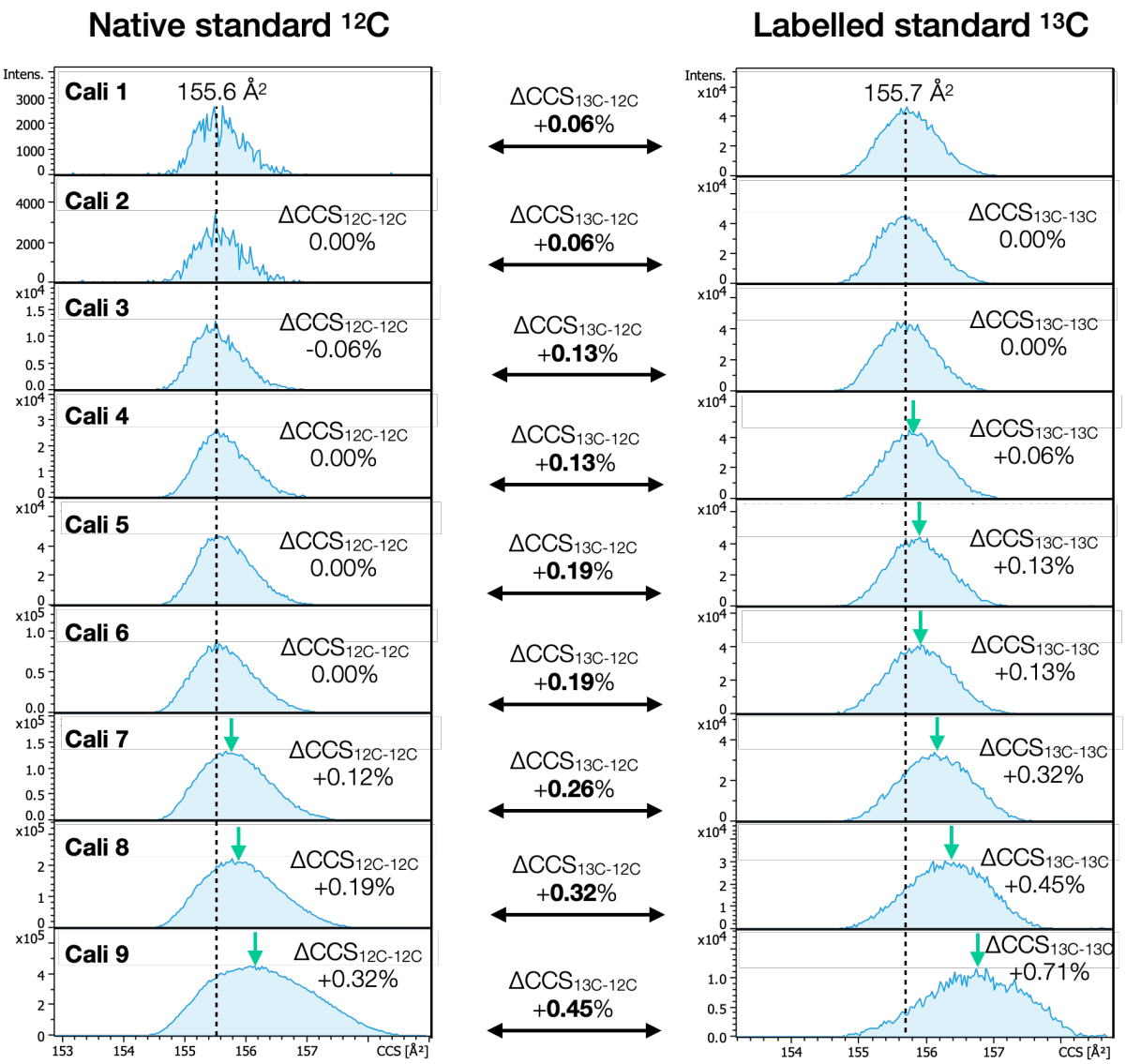

Figure S11: Superposition of the ion mobility spectra of the native and labelled standard of PCB 52 obtained at the different calibration levels. This figure highlights the shift of the ion mobility peaks towards higher CCS values at higher concentration levels for both the native and the labelled standard. It can be seen that the shift occurs earlier and to a greater extent for the labelled standard ($\Delta CCS_{13C-13C}$) compared to the native standard ($\Delta CCS_{12C-12C}$), ultimately resulting in an increase in the CCS difference between native and labelled standard ($\Delta CCS_{13C-12C}$) with increasing concentration levels. Once again, we believe this unequal extent in peak shifts could be attributed to space charge effects.

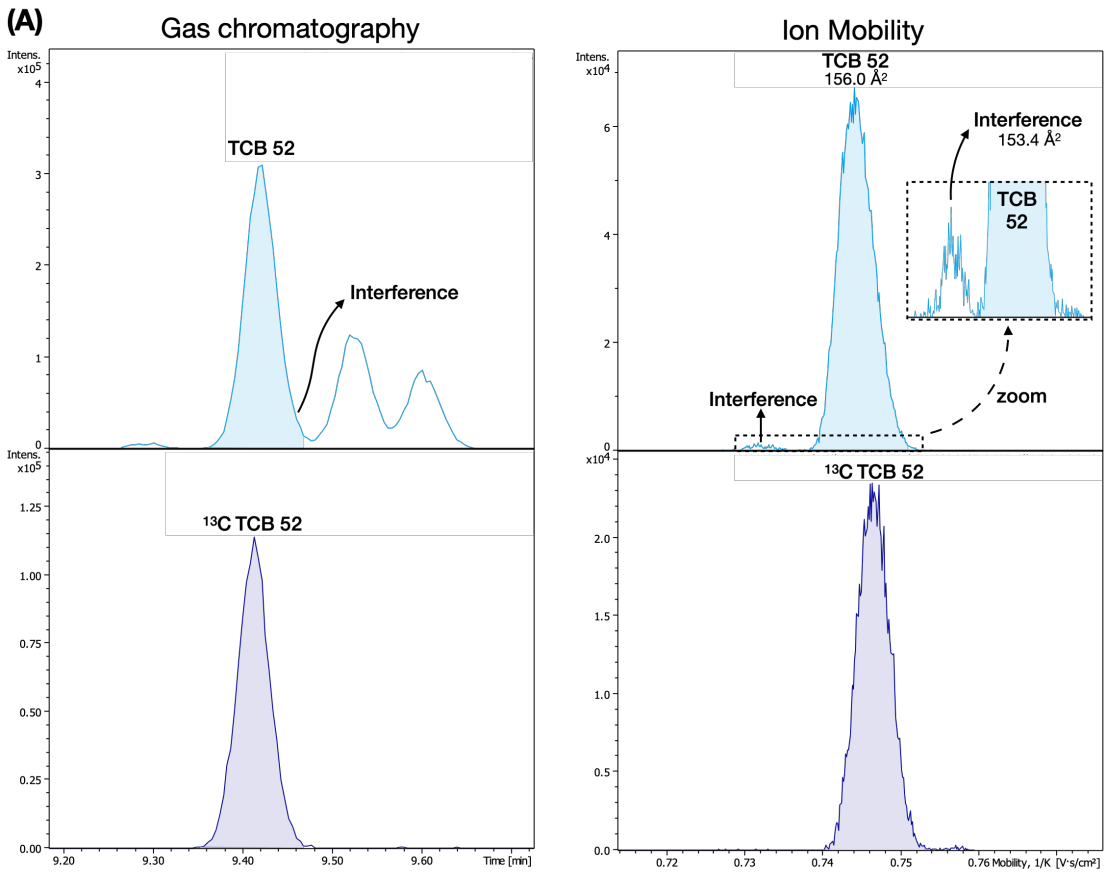
(A)
Gas chromatography
Ion Mobility
TCB 52
Interference
^{13}C TCB 52
TCB 52
156.0 Å²
Interference
153.4 Å²
zoom
Time [min]
Mobility, 1/K [V·s/cm²]

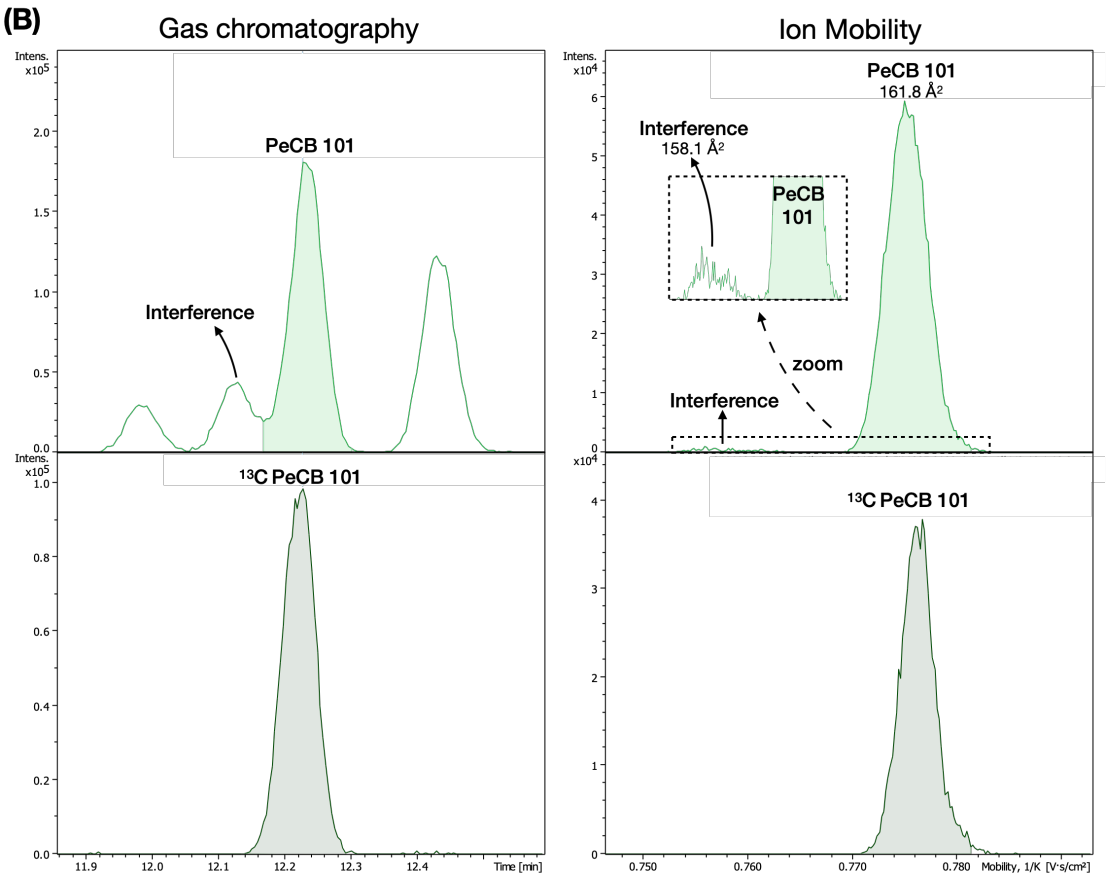
(B)
Gas chromatography
Ion Mobility
PeCB 101
Interference
^{13}C PeCB 101
PeCB 101
161.8 Å²
Interference
158.1 Å²
zoom
Time [min]
Mobility, 1/K [V·s/cm²]

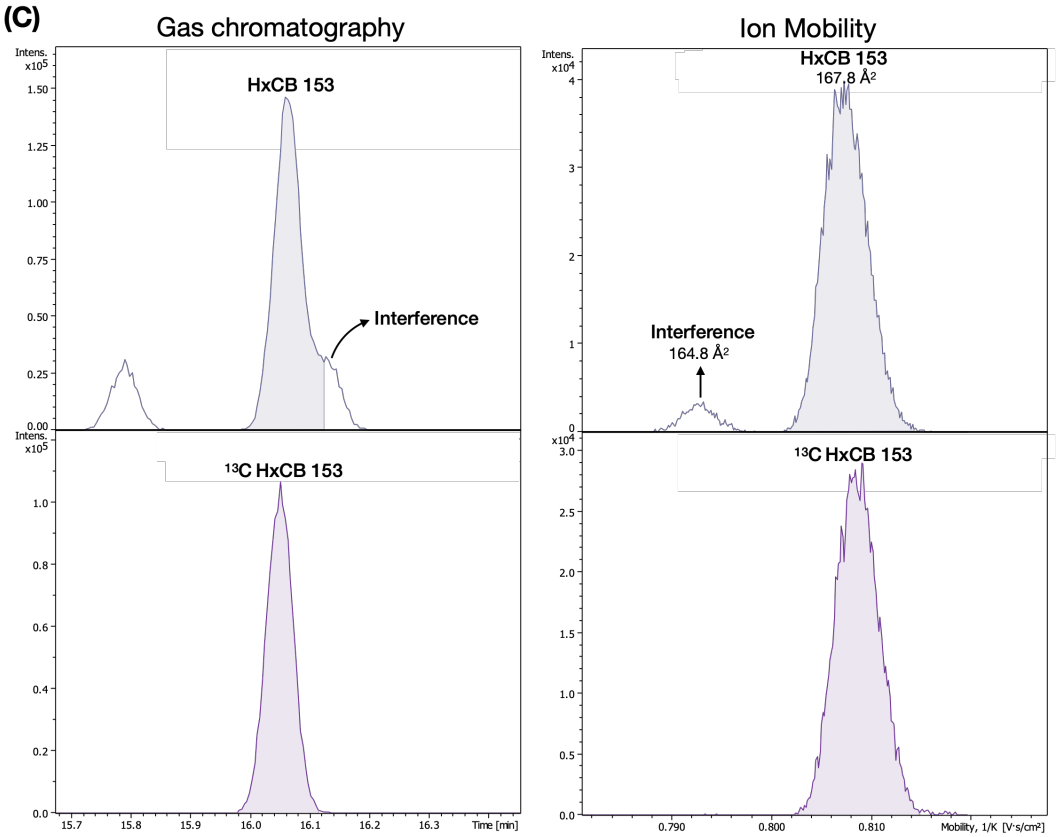

Figure S12: Overlayed chromatograms (left) and ion mobility spectra (right) of native and isotopically labelled standard for (A) TCB 52, (B) PeCB 101 and (C) HxCB 153 (palm oil sample). In each case, the (partially) coeluting isomeric interference in the GC dimension was baseline separated in the ion mobility dimension.

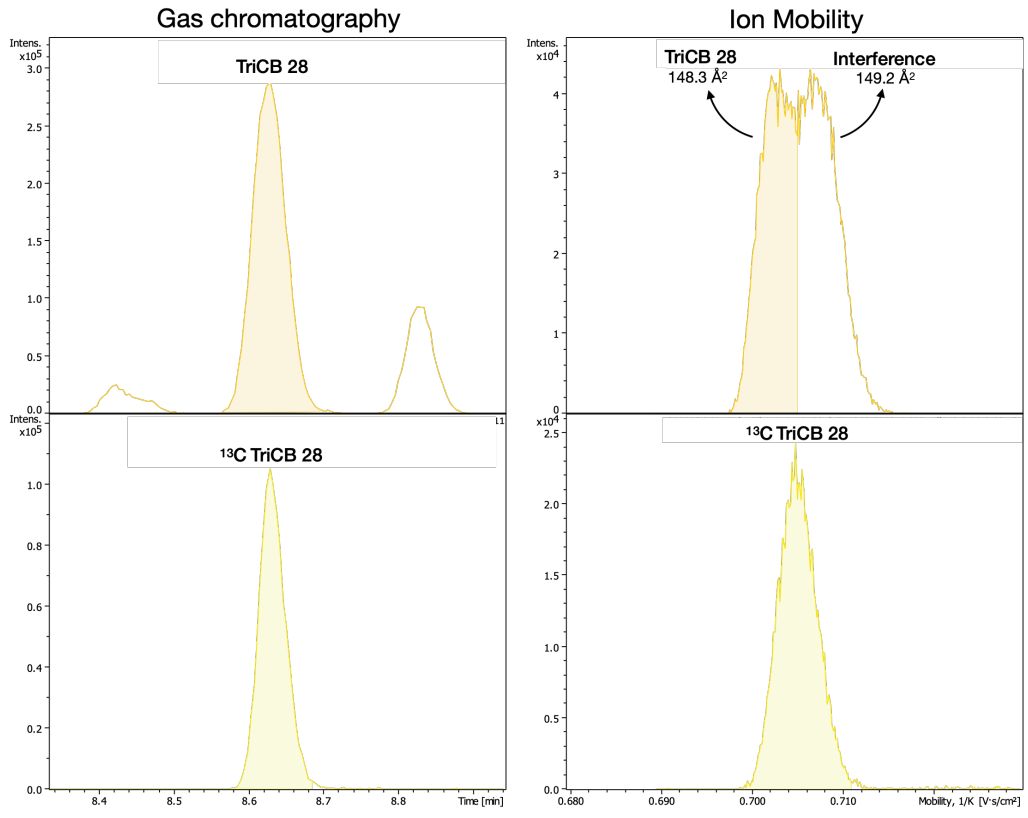

Figure S13: Overlayed chromatograms (left) and ion mobility spectra (right) of native and isotopically labelled standard for TriCB 28 (palm oil sample).

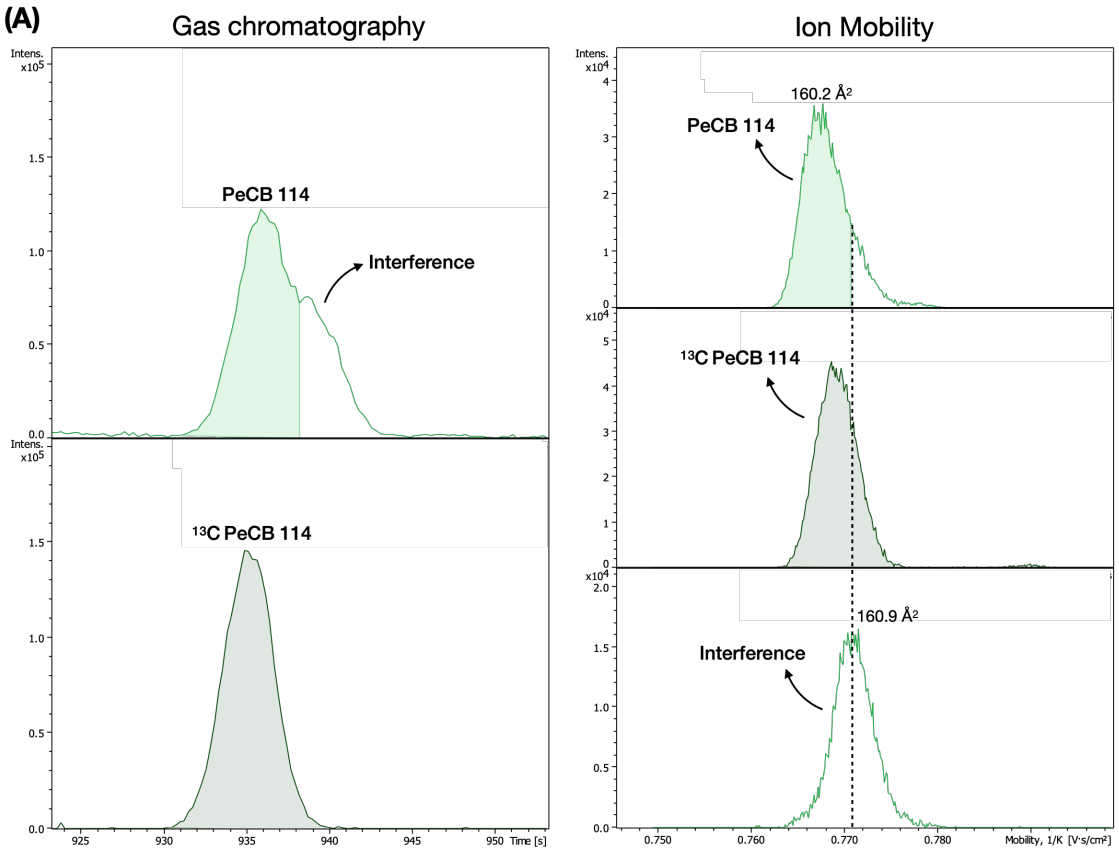
(A)
Gas chromatography
Ion Mobility
PeCB 114
Interference
13C PeCB 114
160.2 Å²
PeCB 114
13C PeCB 114
160.9 Å²
Interference
Time [s]
Mobility, 1/K [V·s/cm²]

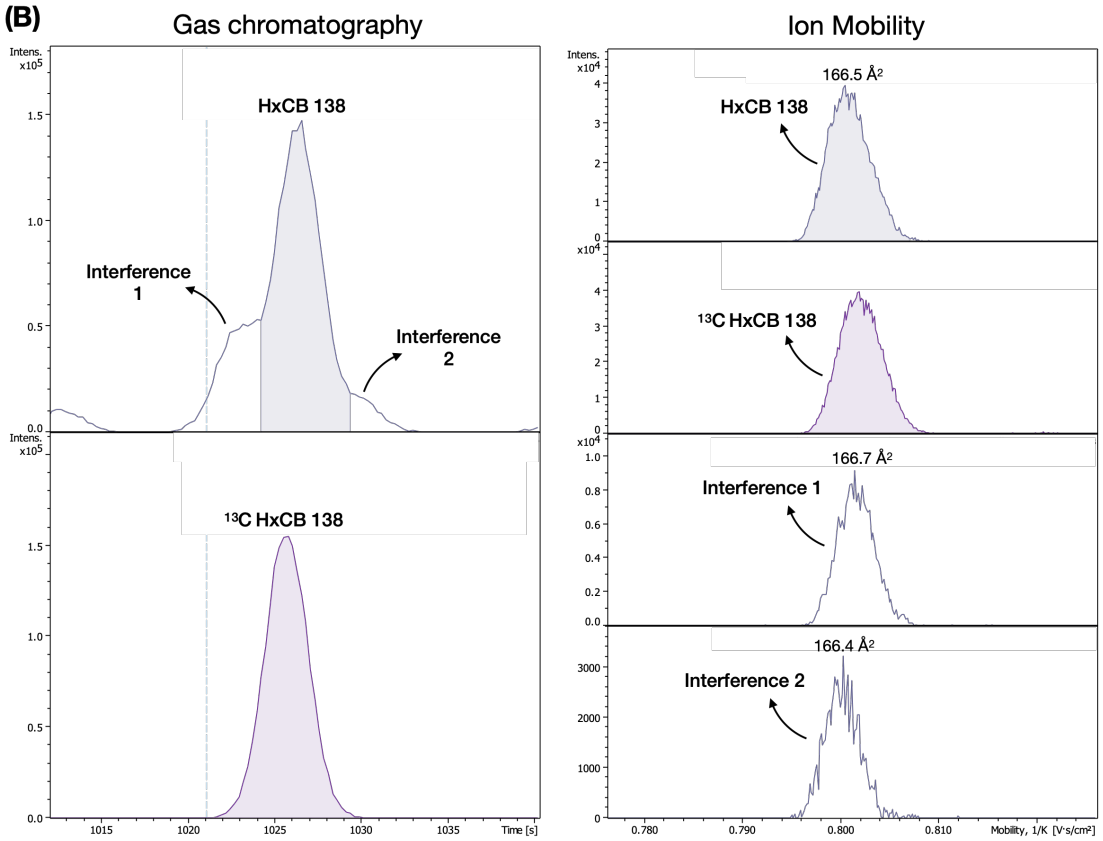
(B)
Gas chromatography
Ion Mobility
HxCB 138
Interference 1
Interference 2
13C HxCB 138
166.5 Å²
HxCB 138
13C HxCB 138
166.7 Å²
Interference 1
166.4 Å²
Interference 2
Time [s]
Mobility, 1/K [V·s/cm²]

(C)

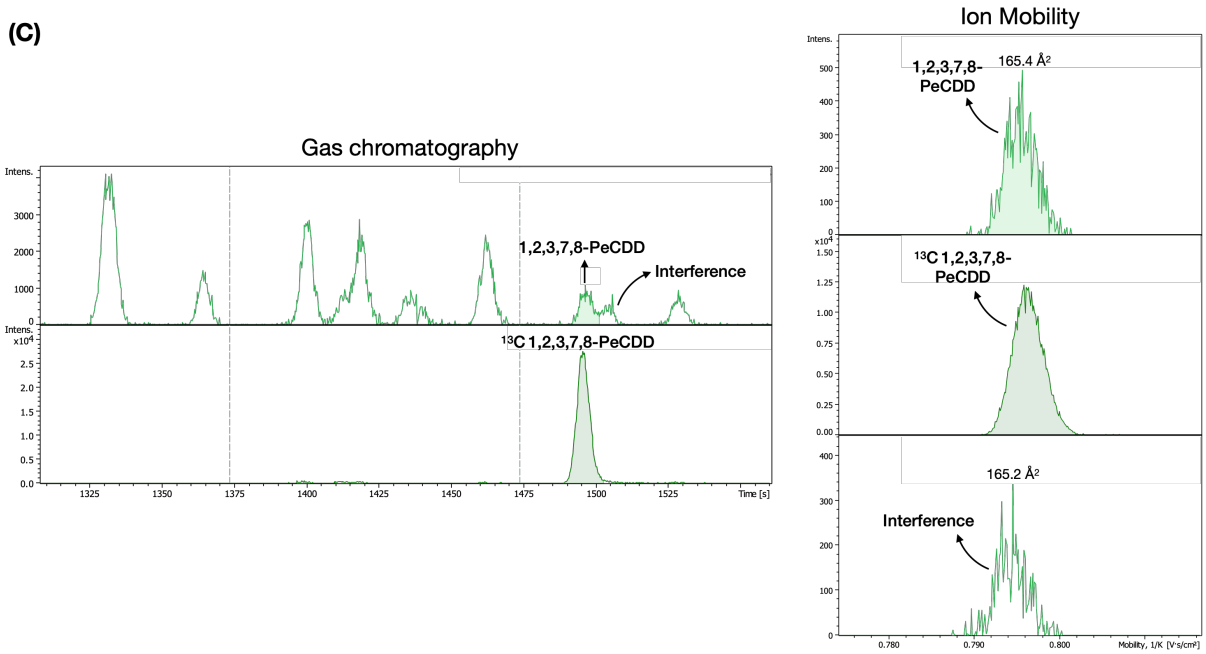
Gas chromatography
Intens.
1,2,3,7,8-PeCDD
Interference
^{13}C 1,2,3,7,8-PeCDD
Time [s]
Ion Mobility
1,2,3,7,8-PeCDD
165.4 Å²
^{13}C 1,2,3,7,8-PeCDD
165.2 Å²
Interference
Mobility, 1/K [V·s/cm²]

(D)

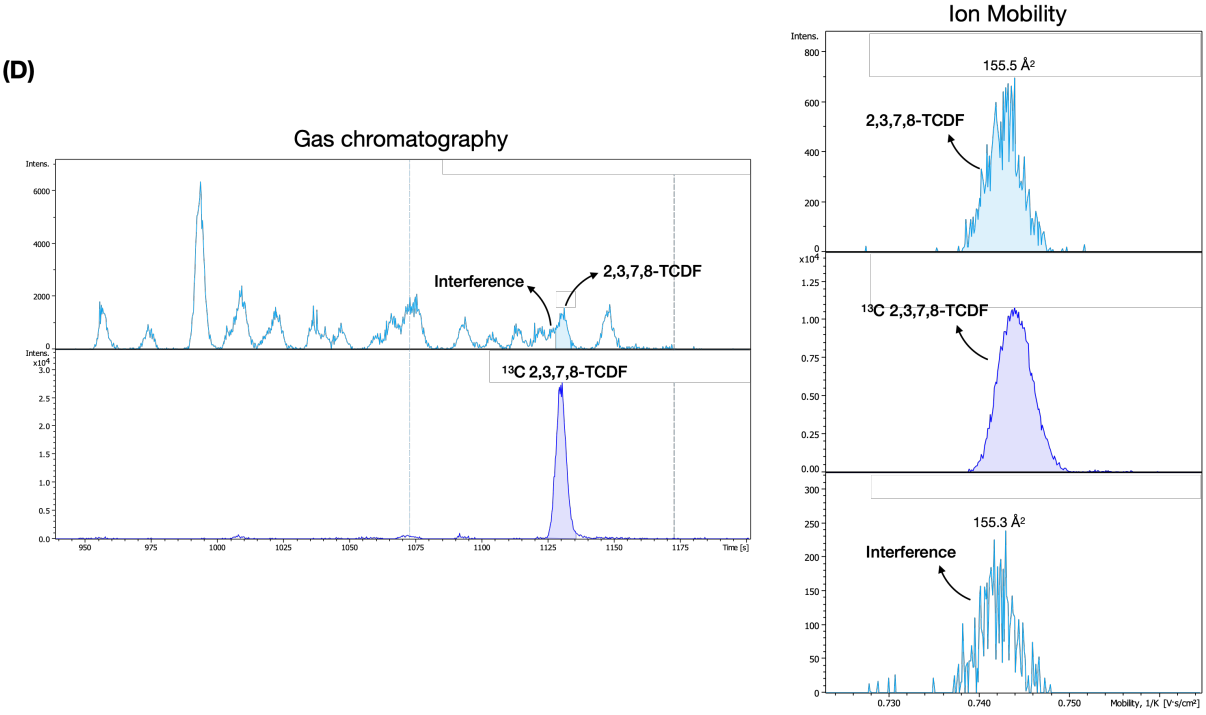
Gas chromatography
Intens.
Interference
2,3,7,8-TCDF
^{13}C 2,3,7,8-TCDF
Time [s]
Ion Mobility
155.5 Å²
2,3,7,8-TCDF
^{13}C 2,3,7,8-TCDF
155.3 Å²
Interference
Mobility, 1/K [V·s/cm²]

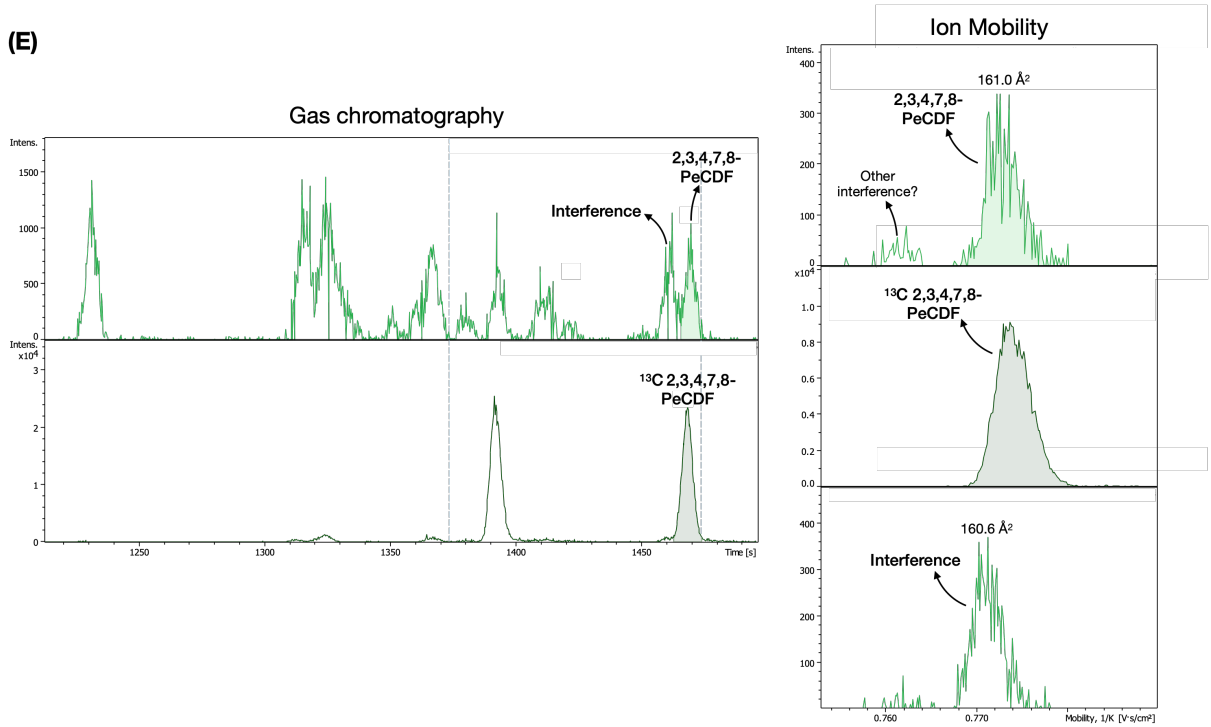

Figure S14: Overlayed chromatograms (left) and ion mobility spectra (right) of native, isotopically labelled standard and interference(s) for (A) PeCB 114 in milk fat, (B) HxCB 138 in palm oil, (C) 1,2,3,7,8-PeCDD in palm oil, (D) 2,3,7,8-TCDF in palm oil and (E) PeCDF 2,3,4,7,8-PeCDF in palm oil. While no significant separation between the analytes and the interferences could be achieved in the IM dimension, most compounds were reasonably separated in the GC dimension. Consequently, the quantification results were not impacted significantly by the presence of these interferences.

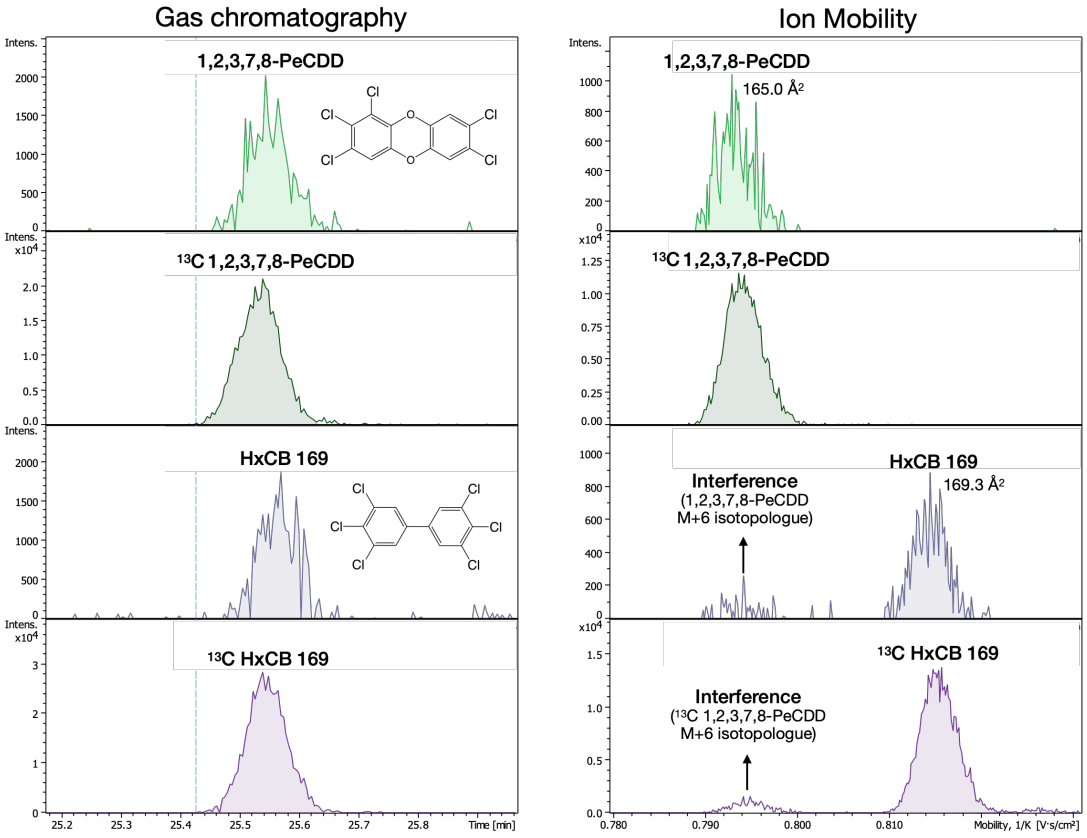

Figure S15: Overlayed chromatograms (left) and ion mobility spectra (right) of native and isotopically labelled standard for the coeluting isobars 1,2,3,7,8-PeCDD and HxCB 169 (milk fat sample).

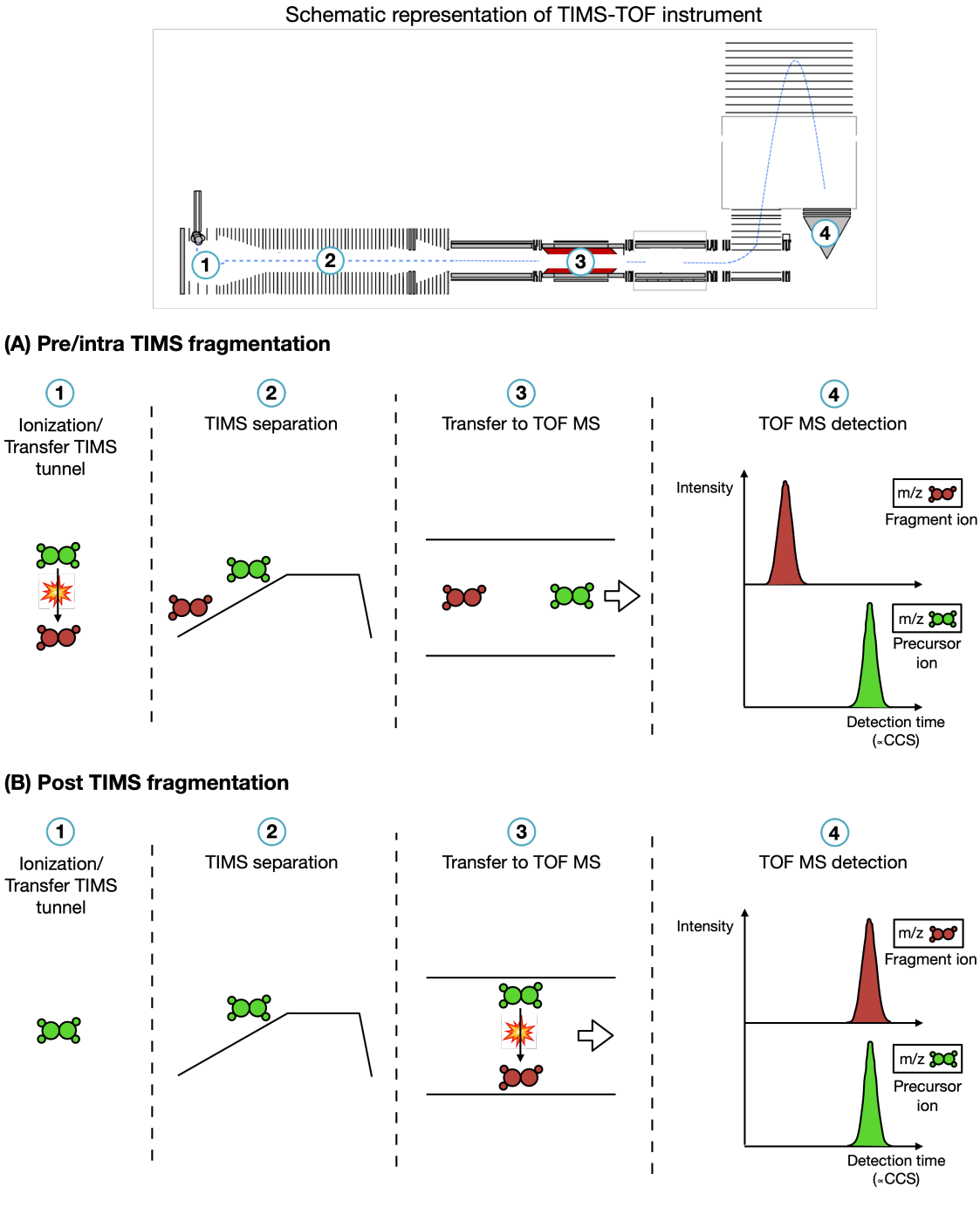

Figure S16: Schematic representation of the TIMS analysis of a parent ion (e.g., $M^{+\cdot}$ or $[M+H]^+$) and its fragment ion (e.g., $[M+H-Cl]^{+\cdot}$ or $[M-Cl]^+$) when fragmentation occurs either **(A)** before/during or **(B)** after TIMS separation. Precursor ions and their fragments are represented in green and red, respectively. In this figure, the TIMS-MS experiment was divided in 4 successive events. The approximate location of a specific event is shown in the schematic representation of the TIMS TOF instrument on top of the figure.

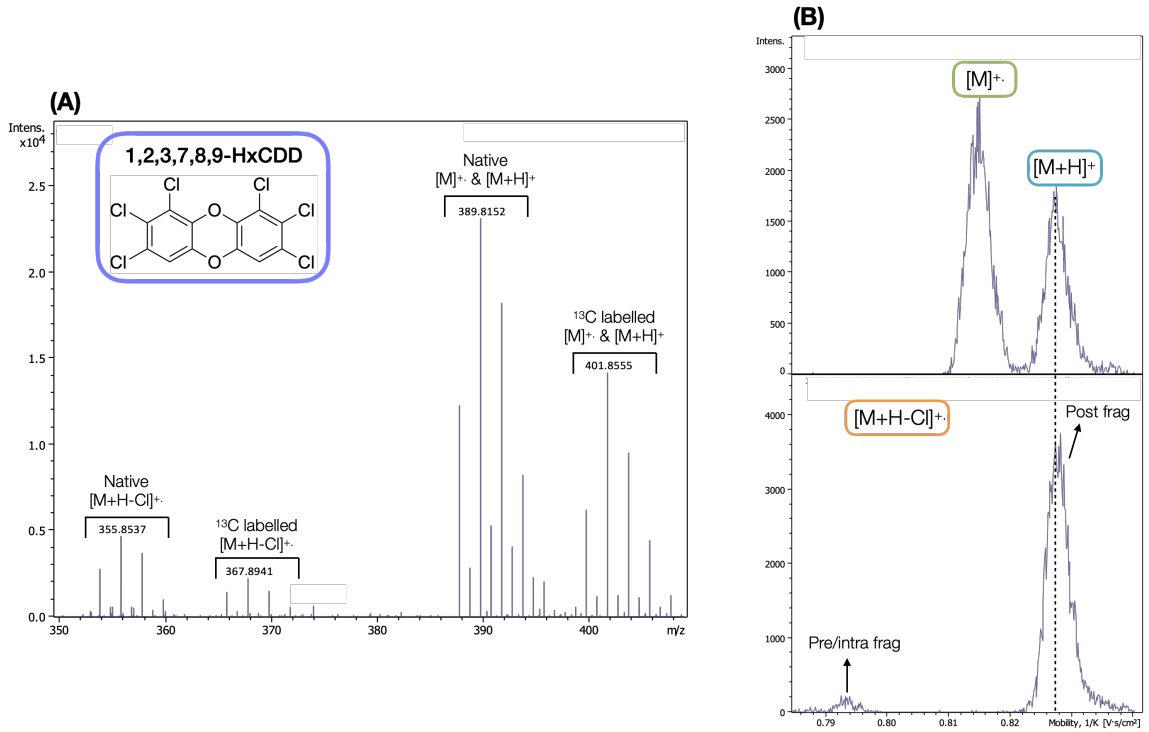

Figure S17: (A) Positive APCI mass spectrum of 1,2,3,7,8,9-HxCDD (from calibration solution level 5). The signal intensity of the $[M+H-Cl]^{+\cdot}$ fragment is about ~20% that of the parent $[M]^{+\cdot}$ Ion. (B) Overlaid ion mobility spectra of the parent ions ($[M]^{+\cdot}$ and $[M+H]^{+}$) and the fragment ion $[M+H-Cl]^{+\cdot}$. The bottom spectra indicate that the great majority of the fragmentation takes place after the TIMS separation. Moreover, the perfect alignment between the $[M+H]^{+}$ peak and the $[M+H-Cl]^{+\cdot}$ "post frag" peak suggest that the $[M+H]^{+}$ ion is the (only) precursor ion that gives rise to the fragment (i.e., the $[M]^{+\cdot}$ ion does not fragment, at least not after the TIMS separation).